User Random Access Delay Optimization in Low-Earth-Orbit Satellite Communication System based on Synchronization Signal Block Periodicity

A Thesis
Presented to
The Academic Faculty

by

Po-Yu Yen

In Partial Fulfillment
of the Requirements for the Degree
Master of Science in the
Graduate Institute of Communication Engineering

National Taiwan University

July 2012

ABSTRACT

Low Earth Orbit (LEO) satellite network has been a promising technology due to the wide spread coverage area and high data throughput. However, with the high speed of satellites, frequent handover is unavoidable for user equipments (UEs) on the ground, causing significant interruption time and signaling overhead. Thus, we introduce a quasi-earth-fixed satellite beam scheme to solve the continually handover from the UEs at the cell edge. In this scheme, we allocate the satellite beams to the ground cells in order to maximize overall throughput. After that, we also propose a UE cell selection algorithm, which base on both position information and UE measurement.

TABLE OF CONTENTS

LIST OF TABLES

LIST OF FIGURES

CHAPTER 1

INTRODUCTION

Non terrestrial network (NTN) has become a promising technique in 6G network. It provides network connectivity to area that traditional network platform cannot reach. For instance, forests, oceans, and deserts. Various platforms are used to provide network services in NTN, such as GEO, MEO, LEO satellites, UAVs, and drones. Among these platforms, LEO is the most actively discussed since it provides global coverage, low latency, and high throughput.

However, to acheive LEO satellite network service, there are some key challanges that need to be resolved. One of the challanges is the unavoidable frequent handover. The high speed of LEO satellite forces user equipments (UEs) on the ground to switch the serving satellites frequently [1]. 3GPP has discussed some solutions to deal with this issue. By using quasi-earth-fixed cell and satellite switch with re-synchronization, the frequent handovers are avoided and the signalling overhead is reduced [2]. Also, with the help of the ephemeris data of satellies and the position information of UEs, the matching between satellites and UEs has been largely improved [3]. Nontheless, it still has some problems during the random access procedure.

CHAPTER 2

BACKGROUND AND RELATED WORK

Related work should be be classified into proper sub-sections depending on the topics related to your thesis research.

2.1 LEO satellite network

2.1.1 Quasi-Earth-Fixed cell

The quasi-Earth-fixed cell is a new non-geostationary satellite orbit (NGSO) satellite beam technique compared to earth-moving cell. Unlike the earth-moving cell that the coverage area of the satellite beam changes when the LEO satellite is moving, the quasi-earth-fixed cell adjusts the beam direction so that the coverage area remains the same in a certain period.

2.2 Random Access Procedure

2.3 Related Work

CHAPTER 3

SYSTEM MODEL

3.1 System Overview

In this paper, we consider a LEO satellite communication system shown in Figure 1. There are N satellites denoted as $\mathcal{N} = \{n \mid n = 1, 2, \ldots, N\}$, and each satellite has M beams denoted as $\mathcal{M} = \{m \mid m = 1, 2, \ldots, M\}$. The coverage area covers K cells on the ground denoted as $\mathcal{K} = \{k \mid k = 1, 2, \ldots, K\}$. There are U user equipments (UEs) in the coverage area denoted as $\mathcal{U} = \{u \mid u = 1, 2, \ldots, U\}$. A hexagonal grid of cells and quasi-earth-fixed cell scheme is considered.

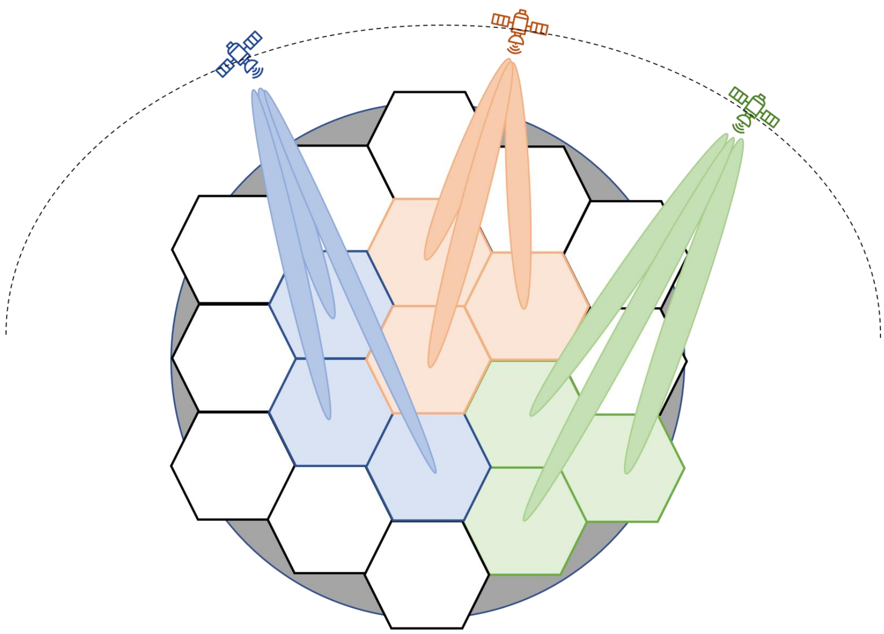

Figure 1: Illustration of satellite beams and cells

3.2 Channel Model

3.2.1 Free Space Path Loss

In the LEO satellite system, the free space path loss from satellite n to cell k can be express as follows [4]:

$$L_{n,k} = \left(\frac{\lambda}{4\pi d_{n,k}} \right)^2 \tag{3.1}$$

where λ is the wavelength,and d is the distance between the n-th satellite and the center of the k-th cell.

3.2.2 Shadowed-Rician Fading Channel

The shadowed-Rician fading model is suitable for satellite communication systems because it accurately reflects the physical propagation environment, capturing both the presence of a strong LoS signal and the effects of shadowing from obstacles [5]. Let $h_{n,k}$ denote the channel gain between the nth satellite and the kth cell. The cumulative distribution function (CDF) of the channel gain:

$$F_{h_{n,k}}(x) = K \sum_{n=0}^{\infty} \frac{(m)_n \, \delta^n \, (2b)^{1+n}}{(n!)^2} \gamma \left(1+n, \frac{x}{2b}\right) \tag{3.2}$$

where $K = (2bm/(2bm+\Omega))^m/2b$, $\delta = \Omega/(2bm+\Omega)/2b$. Ω is the average power of LoS component, and $2b$ is the average power of the multi-path component except the LoS component. m is the Nakagami parameter.

3.2.3 Antenna Radiation Pattern

We introduce the antenna radiation pattern in [6]:

$$G(\theta_{n,m,u}) = G_{max} \left[\frac{J_1\left(\mu(\theta_{n,m,u})\right)}{2\mu(\theta_{n,m,u})} + 36 \frac{J_3\left(\mu(\theta_{n,m,u})\right)}{\mu(\theta_{n,m,u})^3} \right]^2, \tag{3.3}$$

where $\theta_{n,m,u}$ represents the boresight angle between the user position and the beam center with respect to the satellite, G_{max} is the maximum antenna gain, $\mu(\theta) = 2.07123 \cdot \sin(\theta)/\sin(\theta_{3dB})$, where θ_{3dB} is the 3 dB half-power beamwidth angle of the antenna, and $J_1(\cdot)$ and $J_3(\cdot)$ represent the Bessel functions of the first kind of orders 1 and 3.

Thus, with the transmitted power $P_{m,n}$ from the m-th beam of the n-th satellite, the received power from the m-th beam of the n-th satellite to the u-th user $\hat{P}_{n,m,u}$ can be expressed as:

$$\hat{P}_{n,m,u} = P_{n,m} \cdot L_{n,k} \cdot h_{n,k} \cdot G(\theta_{n,m,u}) \tag{3.4}$$

3.3 Synchronization Signal Block Model

Followed by 3GPP protocol [3], the supported synchronization signal block (SSB) periodicity values are {20, 40, 80, 160} miliseconds. Here we define the SSB periodicity of each cell:

$$T_k^{SSB} \in \{20, 40, 80, 160\}, \forall k \in K \tag{3.5}$$

We define the duration of each time slot as 160 ms. To simplify computational complexity, it is assumed that both the positions of the satellites and UEs are fixed within each time slot. Furthermore, the SSB periodicity specification for each cell is considered unchanged throughout the slot.

Let $\Delta_{n,m}[t]$ denote the set of cells served by the m-th beam of the n-th satellite at time slot t. Since the time duration of each slot is 160ms and the SSB periodicity is 20, 40, 80, 160ms, the number of element in $\Delta_{n,m}[t]$ must be 1, 2, 4, or 8, as shown in Figure 2.

T_k^{SSB}	|Δ|	Cell Pattern k							
20	1	1	1	1	1	1	1	1	1
40	2	1	2	1	2	1	2	1	2
80	4	1	2	3	4	1	2	3	4
160	8	1	2	3	4	5	6	7	8
		20ms	20ms	20ms	20ms	20ms	20ms	20ms	20ms

Figure 2: Illustration of satellite beams and cells

3.4 UE Random Access Delay

T_u, the u-th UE random access delay, is defined as the time duration between the u-th UE starts SSB measurement and successfully receives SSB, as shown in Figure 3. T_u can be further decomposed to two parts, T_u^i and T_u^l. T_u^i is defined as the time duration between UE starts SSB measurement and the first SSB arrives. And T_u^l is defined as the time duration between the first SSB arrives to UE succeeds to receive SSB. Since UE can start SSB measurement at any time, T_u^i can be expressed as an uniform distribution random variable $U(0, T_{k_u}^{SSB})$. On the other hand, T_u^l is the multiple of $T_{k_u}^{SSB}$, depending on the number of times the u-th UE fails during random access Q_u. In this thesis, we define that as long as the UE received SSB power is less than P_{th}, the UE will fail to measure SSB. We denote the probability of the received SSB power $\hat{P}_{n,m,u}$ less than P_{th} be P_u^0. The mathematical formula can be expressed as follows:

$$T_u = T_u^i + T_u^l \tag{3.6}$$

$$F_{T_u^i}(t) = \begin{cases} \frac{t}{T_{k_u}^{SSB}}, & 0 \leq t < T_{k_u}^{SSB} \\ 1, & t \geq T_{k_u}^{SSB} \\ 0, & \text{otherwise} \end{cases} \tag{3.7}$$

$$T_u^l = Q_u \cdot T_{k_u}^{SSB} \tag{3.8}$$

$$\Pr\left[Q_u = n\right] = (1 - P_u^0)(P_u^0)^n \tag{3.9}$$

where k_u is the cell where the u-th UE is located.

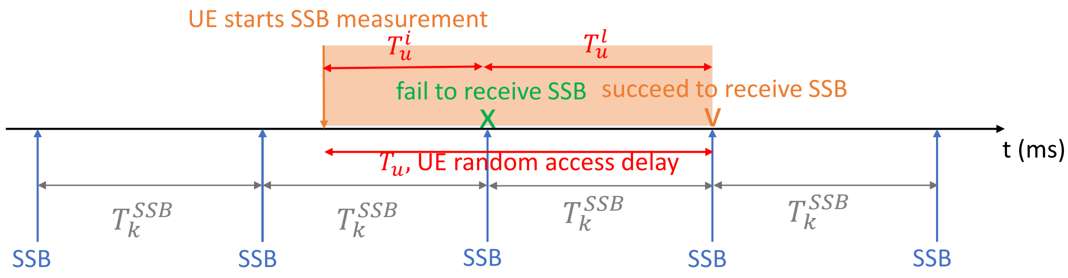

Figure 3: Illustration of UE random access delay

3.5 Problem Formulation

During the latest 3GPP meeting, the adjustment and implementation of SSB periodicity in the NGSO scenario were discussed intensively. In the 3GPP RAN1 #116 meeting [7], further specifications for the LEO satellite communication scenario were defined. This raises an important issue: How can satellites provide random access to such a large number of cells with limited power? It is clear that if we extend the SSB periodicity for some cells, the satellites' power consumption is reduced, while the UE random access delay increases. The transmitted power of the SSB also affects the success probability of the random access procedure between satellites and UEs. Thus, this thesis will investigate the trade-off between power allocation, SSB periodicity, and UE random access delay, which can be described by the following mathematical model:

$$
\begin{aligned}
&\min_{\Delta, P_{n,m}} \sum_{U} T_u \\
&\text{subject to} \\
&\quad \sum_{m} P_{n,m}[t] \leq P_s, \quad \forall n \in \mathbb{N} \\
&\quad \Delta_{n,m}[t] \in \{0,1,2,4,8\}, \quad \forall n \in \mathbb{N}, m \in \mathbb{N} \\
&\quad \Delta_{n,m}[t] \cap \Delta_{n',m'}[t] = \emptyset, \quad \forall n, n' \in \{1,2,\ldots,N\}, m, m' \in \{1,2,\ldots,M\}, (n,m) \neq (n',m')
\end{aligned}
\tag{3.10}
$$

where P_s is the maximum transmitted power for each satellite.

CHAPTER 4

PROPOSED ALGORITHM

CHAPTER 5

PERFORMANCE EVALUATION

All figures should be of the same width whenever possible for consistency.

5.1 Simulation Setup

We use BONMON [**?**] to solve the optimization problem. The simulation setup follows that in [**?**].

5.2 Simulation Results

CHAPTER 6

CONCLUSION AND FUTURE WORK

REFERENCES

[1] "Solutions for nr to support non-terrestrial networks (ntn)," 3rd Generation Partnership Project (3GPP), Technical Report TR 38.821, 2023, release 16. Online Available at: https://www.3gpp.org/dynareport/38821.htm

[2] "Nr; nr and ng-ran overall description; stage-2," 3rd Generation Partnership Project (3GPP), Technical Specification TS 38.300, 2024, release 18. Online Available at: https://www.3gpp.org/dynareport/38300.htm

[3] 3GPP, "Radio Resource Control (RRC) protocol specification," 3rd Generation Partnership Project (3GPP), Technical Report TR 38.331, March 2024, version 18.1.0. Online Available at: https://www.3gpp.org/ftp/Specs/archive/38_series/38.331/

[4] J. Wang, C. Jiang, L. Kuang, and R. Han, "Satellite multi-beam collaborative scheduling in satellite aviation communications," *IEEE Transactions on Wireless Communications*, vol. 23, no. 3, pp. 2097–2111, 2024.

[5] D.-H. Jung, J.-G. Ryu, W.-J. Byun, and J. Choi, "Performance analysis of satellite communication system under the shadowed-rician fading: A stochastic geometry approach," *IEEE Transactions on Communications*, vol. 70, no. 4, pp. 2707–2721, 2022.

[6] S.-H. Chen, L.-H. Shen, K.-T. Feng, L.-L. Yang, and J.-M. Wu, "Energy-efficient joint handover and beam switching scheme for multi-leo networks," in *2024 IEEE 99th Vehicular Technology Conference (VTC2024-Spring)*, 2024, pp. 1–7.

[7] 3GPP TSG RAN WG1, "Final report of 3gpp tsg ran wg1 #116 v1.0.0," 3rd Generation Partnership Project (3GPP), Athens, Greece, Technical Report R1-2400000, February 2024, meeting held February 26th – March 1st, 2024. Online Available at: https://www.3gpp.org/ftp/tsg_ran/WG1_RL1/TSGR1_116/Report/Final_Report_3GPP_TSG_RAN_WG1_116_v1.0.0.pdf